15TH IEA HEAT PUMP CONFERENCE
MAY 26–29, 2026 | HOFBURG
VIENNA 2026
DECARBONISATION THROUGH INNOVATION

Rotary gas pressure exchanger for expansion work recovery & efficiency improvement in trans-critical CO2 heat pumps

Azam Thatte[a*], Choon Tan[b], Brian Fricke[c], Kashif Nawaz[c]

[a]Energy Recovery, Inc., 1717 Doolittle Dr., San Leandro, CA 94577, USA.
[b]Massachusetts Institute of Technology, 77 Massachusetts Ave., Cambridge, MA 02139, USA.
[c]Oak Ridge National Lab, 1 Bethel Valley Rd., Oak Ridge, TN 37830, USA.

Abstract

Heat pumps with CO2 as the working fluid provide unique advantages and facilitates transition away from global warming hydrofluorocarbons (HFC) towards natural refrigerants with ultra-low global warming potential. However, the molecular structure of CO2 causes the heat rejection pressure to be much higher compared to HFCs, resulting in lower efficiency of the cycle at high gas cooler exit temperatures. Exergy and second law analysis indicates that largest fraction of exergy is destroyed during the throttling process over high differential pressure between heat source and sink. To increase exergetic efficiency, this paper presents a novel rotary gas pressure exchanger (RPX), which allows expansion work recovery using direct fluid-to-fluid contact acoustic pressure exchange between high pressure supercritical CO2 and low pressure gaseous CO2. RPX facilitates both, the compression and the expansion using acoustic waves generated in a compact high speed axially ducted rotary machine. RPX can compress a large fraction of the low pressure CO2 vapor for free without consuming any external mechanical or electrical energy, but rather through the expansion work recovery. This expansion work recovery, not only reduces the exergy destruction during expansion process but also provided free subcooling, thus reducing total system mass flow for same amount of total heat delivered or delivering more heat for same amount of compressor work consumed. Test results demonstrate more than 95% pressure recovery coefficient and no-pass through characteristic of mass transport through RPX. The paper presents a novel RPX integrated heat pump architecture that shows up to 16% COP improvement achieved through this reduction in exergetic efficiency of the cycle. Such an RPX integrated heat pump architecture has a great potential to facilitate efficient decarbonization of district and industrial process heat using ultra-low global warming refrigerants like CO2.

Keywords: Trans-Critical CO2 Heat Pumps; Rotary Gas Pressure Exchanger, Efficiency; Exergy;Expansion Work Recovery

1. Introduction

The thermodynamic landscape of modern refrigeration / heat pump systems is undergoing a paradigmatic shift, moving from synthetic hydrofluorocarbons (HFCs) like R134a toward natural refrigerants, specifically Carbon Dioxide (CO2). This transition is driven by the urgent need to reduce Global Warming Potential (GWP); CO2 possesses a GWP of 1, whereas R134a stands at 1,430. CO2 has recently emerged as one of the most attractive choices for low global warming, low ozone depleting, non-toxic, non-flammable refrigerant. It has GWP =1, ODP=0, it is non-toxic, unlike Ammonia and non-flammable unlike Propane. CO2 has some very favorable thermo-physical properties as a refrigerant, e.g. the latent heat of evaporation of CO2 is relatively large (still lower than Ammonia) but the saturation pressure for CO2 at typical evaporating temperatures needed in refrigeration is much higher, which increases its density and thus makes the volumetric flow much smaller for the same heat absorption capacity as other refrigerants. This makes the refrigeration capacity per unit volume for CO2 about 4 times that of R410A, ~5 times that of Ammonia, ~6 times that of Propane and ~ 8 times that of R134a, R600a and R152a. In supercritical state, CO2's specific heat is very high, it has high thermal conductivity and low kinematic viscosity. These properties provide it high Nusselt number and thus excellent heat transfer efficiency and thermal transport characteristics. Additionally, due to higher evaporating and condensing / gas cooler pressures, the energy density of CO2 is much higher, which in turn reduces the pipe diameters by ~ 30% compared to traditional refrigerants. Higher suction density also reduces the volumetric size of the compressors, making them much compact. The adoption of CO2 is not merely a chemical substitution; it requires a fundamental re-engineering of thermodynamic cycles due to operating pressures that are an order of magnitude higher than conventional systems. The condensing pressures for various refrigerants are shown in Fig. 1(a). Above its critical temperature of 31 deg. C, CO2 does not condense and hence the pressure under this scenario is the “optimal” gas cooler pressure required to maximize COP of the refrigeration / heat pump cycle.

Due to its molecular structure compared to refrigerants like Ammonia and HFCs, there are some unfavorable properties that work against CO2. The saturation pressure of CO2 for a given temperature is much higher than that for HFCs or NH3. The reason why the condensing or gas cooling pressure of CO2 is significantly higher than other refrigerants has origins in quantum chemistry and in the molecular structure of CO2. CO2 is a non-polar molecule, unlike NH3. The dipole-dipole interaction between NH3 molecules creates more affinity towards each other and produces strong inter-molecular forces. The non-polar nature of Carbon Dioxide, driven by its linear symmetry and cancellation of dipole moments, results in weak London dispersion forces. These weak intermolecular attractions result in high volatility and a uniquely low critical temperature (30.98 deg. C). To understand the thermodynamic parameters of CO2, one must first analyze the quantum mechanical arrangement of the molecule. The macroscopic property of "pressure" is essentially the aggregate statistical result of molecular collisions and intermolecular repulsions/attractions. In the case of CO2, the lack of strong cohesive forces between molecules is the primary driver for the high pressures required to condense CO2 into liquid state.

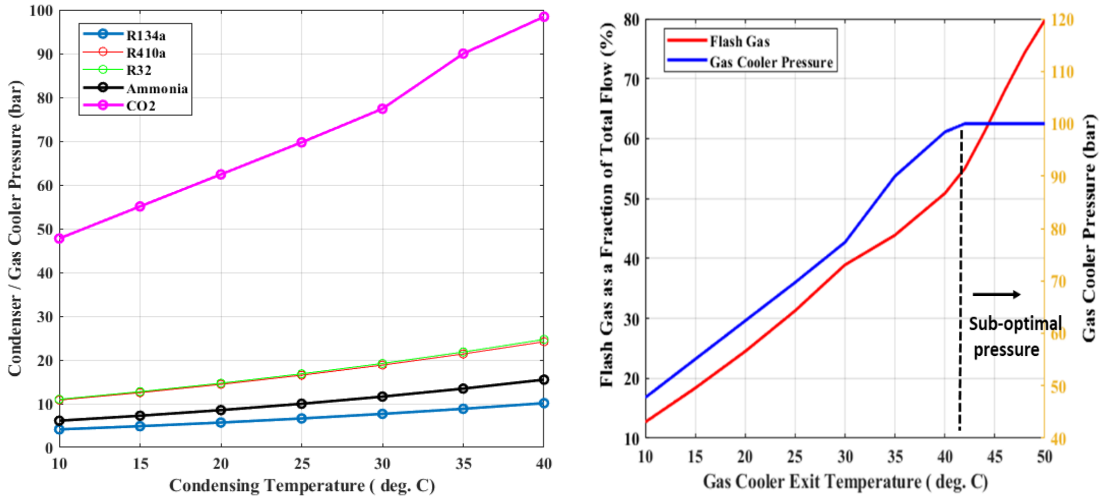

(a) (b)

Figure 1. (a) Condensing pressure for various refrigerants. Above 31 deg. C, CO2 does not condense and hence the pressure under this scenario is the “optimal” gas cooler pressure required to maximize COP of the refrigeration / heat pump cycle. (b) Flash gas produced in CO2 heat pumps increases sharply as gas cooler pressure gets constrained.

Additionally, the strongly positive hydrogen atom in NH3 gets attracted to negatively charged Nitrogen atom from a neighboring molecule creating a strong intermolecular force. Similar strong inter-molecular forces exist in hydro-fluoro-carbon (HFC) molecules. Stronger the inter-molecular force, lesser the pressure required to keep molecules together in a liquid state, and thus lower the saturation pressure. CO2 on the other hand is non-polar and does not have a hydrogen atom and hence has much lower inter-molecular forces of attraction and thus molecules are easy to float away from each other, forming a gaseous state. The pressure required to keep molecules together in a liquid form is thus higher and hence the saturation pressure of CO2 is much higher than NH3 and HFC refrigerants at the same temperature.

Higher saturation pressure means the heat rejection pressure (condensing pressure) for CO2 is much higher than HFCS or NH3 (e.g. 66 bar at 27 deg. C for CO2 as opposed to 10 bar for NH3 at same temperature). Further, the critical temperature for CO2 is lowest of all currently used refrigerants (31 deg. C compared to

132.4 deg. C for NH3, 101.1 deg. C for R134a) which means for warmer climates where temperature would be higher than 31 deg. C, CO2 inside the condenser will be in supercritical state and will no longer condense. Since CO2 does not condense, the gas cooler pressure and temperature become independent of each other (unlike in subcritical heat rejection where pressure is always equal to the saturation pressure). This requires the CO2 system to find an "optimal" gas cooler pressure for temperatures above the critical temperature. Such an optimization is carried out by mathematically minimizing the COP of the system with respect to gas cooler pressure, i.e. by making sure the first derivative of COP function with respect to gas cooler pressure is zero and the second derivative is negative. The value of the gas cooler pressure that satisfies these two constraints ensures the maximum efficiency for the CO2 refrigeration or heat pump cycle. As can be seen from Fig.1(a), the optimal gas cooler pressure for CO2 system found in this manner is very high and often times the system operator puts restrictions on the maximum pressure allowed in the system based on safety regulations, cost considerations for high pressure piping as well as the compressor discharge pressure and discharge temperature limitations. For example, often times the maximum compressor discharge pressure is limited to 100 bar. When the gas cooler pressure gets constrained in such a manner, the amount of flash gas produced after expansion through HPV increases non-linearly with increase in gas cooler exit temperature. This is shown in Fig. 1(b). Since flash gas does not contribute anything to the heat absorption, this non-linearly increase in flash gas at higher temperatures increases energy consumption of compressor proportionately for same amount of heat absorbed in the evaporator. This causes the system COP (efficiency) to reduce dramatically at higher ambient temperatures and makes it progressively more expensive to operate in warmer climates. This is one of the key challenges of CO2 refrigeration / heat pump systems.

To remedy this issue, this paper introduce a novel device called Rotary Gas Pressure Exchanger (RPX) that does "expansion work recovery" and compresses part of the total heat pump system flow without using any external mechanical or electrical energy. We also design a new heat pump system architecture that incorporates RPX either to compress the flash gas or to reduce the flash gas produced using an RPX facilitated subcooling mechanism. These are discussed in next sections.

2. Methods

2.1. Exergy Analysis of CO2 Heat Pump System

We start by performing thermodynamic system analysis of a simple 4-component (evaporator, compressor condenser/gas cooler and expansion valve) heat pump cycle operating between low temperarature Tsource and high temperature Tsink and T_0 as the reference (ambient) temperature. We conduct the first law (energy balance) and second law (exergy analysis) thermodynamic investigation. The exergy destruction in each of these four components can be given by Eq.(1) through Eq. (4) respectively.

$$Exd_{Evap} = \dot{m}\left[\left(h_4 - h_1\right) - T_0\left(s_4 - s_1\right)\right] + Q_L\left(1 - \frac{T_0}{T_{Source}}\right) \tag{1}$$

$$Exd_{Comp} = \dot{m} \cdot T_0 \cdot \left(s_2 - s_1\right) \tag{2}$$

$$Exd_{Gas\,Cooler} = \dot{m}\left[\left(h_2 - h_3\right) - T_0\left(s_2 - s_3\right)\right] - Q_H\left(1 - \frac{T_0}{T_{\mathrm{Sin}\,k}}\right) \tag{3}$$

$$Exd_{ExpValve} = \dot{m} \cdot T_0 \cdot \left(s_4 - s_3\right) \tag{4}$$

Such an exergy analysis provides the insights into the locations of inefficiencies in the heat pump system. We then analyse the variation of exergy destroyed in each of the above components as a function of gas cooler exit temperature for a fixed source temperature (i.e. evaporating temperature) to understand how the entropy generation in each of these 4 processes varies with increasing condensing /gas cooler exit temperature. We then rank the relative contribution of each component of the system to the overall exergy destruction of the cycle to highlight the highest source of inefficiency in the CO2 heat pump cycle. The results of this analysis are shown in section 3. .

2.2. 3D Multi-Phase Flow Model of Rotary Gas Pressure Exchanger

Figure 2 shows the RPX schematic. It features a high-speed rotor with axial ducts that spins inside a sleeve, held between two end caps by a thin hydrodynamic/hydrostatic gas film. This setup allows the rotor to spin at high speeds without mechanical thrust or radial bearings, as the gas film provides both axial and radial support and acts as a seal between pressure sides. Viscous friction losses from the gas film are much lower than those of contact-type bearings. The operation of RPX consists of various stages of compression, sealing and expansion during one rotation.

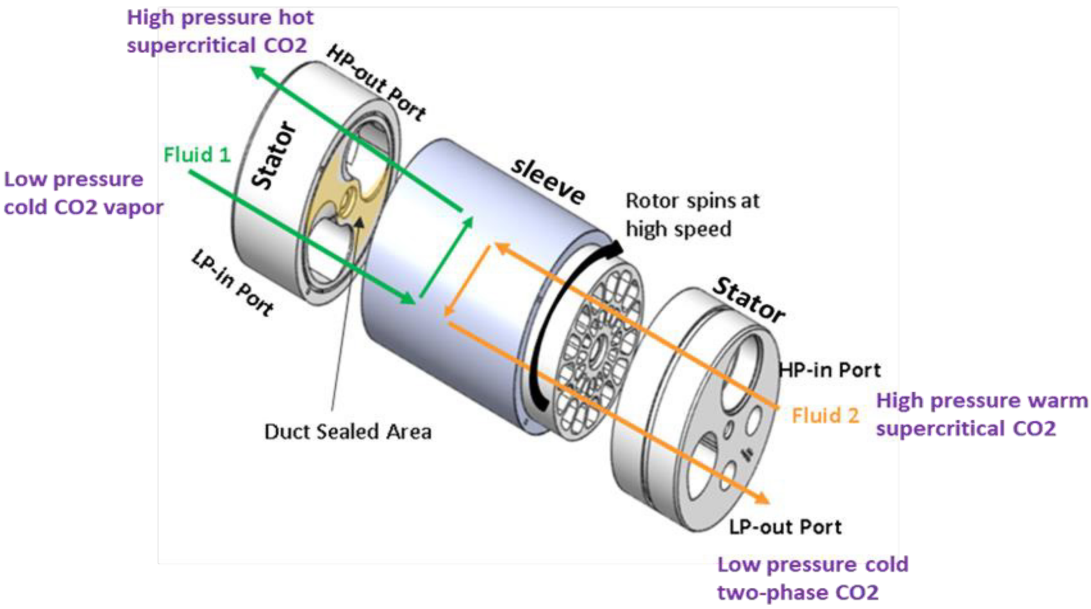

Figure 2. Geometry of RPX with two inlet and two exit fluid streams.

Two fluid streams, at two different pressures and thermodynamic states enter the rotor from axially opposite ports (HPin port and LPin port). They come in direct contact with each other for a short duration (few milliseconds) inside the rotating duct. As the duct rotates and the low-pressure (LPin) fluid is exposed to the high-pressure port, an acoustic wave is generated, rapidly pressurizing the LP fluid at a rate determined by the velocity of the acoustic wave. During stage 1, LP CO2 vapor enters through the LPin port and occupies the PXG rotor duct. The parameter LPinTD denotes a non-dimensional volumetric flow rate of the LP fluid representing the fraction of the duct length filled by this fluid plug. As the LP fluid fills a portion of the duct corresponding to LPinTD, it displaces residual fluid 2 from the previous cycle. A minor diffusion mixing zone exists between fluid 1 and fluid 2 inside the duct; however, careful design minimizes this zone, ensuring it remains within the duct and does not exit. Consequently, fluid 1 never leaves via LPout port, as confirmed later in the paper by results from the 3D species transport CFD model.

As the duct continues to rotate, fluids 1 and 2 are sealed between the land areas of the two end caps (stage 2), preventing significant mass transfer into or out of the duct. When the duct becomes exposed to the HPout port, an instantaneous acoustic wave propagates through the duct, compressing fluid 1 to match the pressure of high-pressure fluid 2. This compression process increases the temperature of fluid 1 through an isentropic-like transformation with a defined isentropic efficiency. The density of the LP fluid plug, now at high pressure (HP), rises, causing its volume to decrease while its contained mass remains constant. A small amount of thermal energy transfer occurs between the two fluids as they come in direct contact. During this phase, the now hotter fluid 1 relinquishes part of the enthalpy acquired during compression to fluid 2. The extent of heat transfer depends on the specific heat capacities, heat transfer coefficients, densities, and thermal conductivities of the respective fluid plugs, as well as the duration before the subsequent stage (stage 3) commences. This time interval is governed by the rotor'rotational speed.

As the duct continues its rotation, it fully aligns with both the HPin and HPout ports, marking the start of stage 3. At this point, high-pressure fluid 2, such as supercritical CO_2 from the gas cooler exit, enters the rotor via the HPin port and fills a section of the duct corresponding to the HPin travel distance (HPinTD). This

HPinTD represents a non-dimensional volumetric flow rate, normalized by the rotor's total duct volume and its rotational speed. When the plug of HPin fluid flows into the duct, it displaces the plug of LPin fluid at an equal volumetric flow rate. However, since the LPin plug has undergone compression, its density differs from that of both incoming HPin and original LPin fluid, depending on its temperature. This density determines the mass flow rate of the fluid exiting the HPout port under high pressure and in the supercritical state.

Further duct rotation triggers stage 4, sealing the duct again; but now at high pressure. As soon as the duct is exposed to the LPout and LPin ports, an acoustic expansion wave emerges, causing depressurization via a process akin to isentropic expansion, governed by isentropic efficiency. This expansion phase shifts the HPin fluid plug inside the duct from a supercritical state to a two-phase liquid-gas mixture. The quality (gas mass fraction) of this CO2 mixture depends on the isentropic expansion efficiency, generally resulting in a higher liquid content than an isenthalpic expansion, such as through a throttle valve.

In the next stage, the two-phase liquid-gas plug briefly exchanges heat with the LPin fluid plug. During these few milliseconds, a small portion of the liquid may vaporize due to limited residence time. The resulting mixture, at the saturation temperature for LP pressure, exits through the LPout port.

To investigate above gas dynamics taking place inside RPX rotor that leads to pressure exchange between high pressure supercritical CO2 and low pressure gaseous CO2 through acoustic waves, a 3D multi-phase CFD model was developed. The model also tries to capture the species transport and mixing between incoming HP supercritical CO2 stream and LP gaseous CO2 stream. The details of this CFD model are described by the author previously ([5]). Further, a transport equation for scalars in a given phase is written and solved along with the Navier Stokes equations in ANSYS CFX. Eq. (5) shows this transport equation for kth scalar field in each of the phases "n". The solution algorithm solves this transport equation inside the volume occupied by the nth phase.

$$\frac{\partial\left(\alpha_n \rho_n \phi_n^{\,k}\right)}{\partial t} = \Psi_n^{\,k} + \nabla\cdot\left(\alpha_n D_n^{\,k} \nabla \phi_n^{\,k}\right) - \nabla\cdot\left(\alpha_n \rho_n \vec{u}_n \phi_n^{\,k}\right) \tag{5}$$

2.3. RPX Integrated Trans-Critical CO2 Heat Pump Architectures

Having investigated the performance of RPX through the high fidelity 3D fluid-thermal-species transport model described in section 2.2, next a new type of heat pump system architecture integrated with this RPX is developed. A schematic of this system is shown in Fig. 3. In this system a portion (e.g. 10-15%) of the flow exiting the gas cooler is bypassed through a bypass valve and undergoes expansion. The cold two phase liquid-vapor mixture thus created then exchanges heat with the remaining 85-90% of the main gas cooler exit flow in a subcooler. This cools the primary flow down before expanding through the RPX from HPin port to LPout port. RPX recovers expansion work during this expansion process and thus, this expansion through RPX produces more liquid mass fraction than the standard isenthalpic expansion through a high pressure expansion valve of the typical heat pump cycle, thus reducing the total mass flow required per unit heat absorbed in the evaporator. Further, RPX uses this expansion work recovered to compress the low pressure bypass flow exiting the subcooler to the highest pressure in the system (i.e. gas cooler pressure), without consuming any external electrical or mechanical energy. Thus, in effect, RPX facilitates "free subcooling" of the gas cooler exit flow without needing an electrically driven "mechanical subcooler compressor". As a result, the flash gas produced by the system is significantly reduced and thus reducing the main compressor's power consumption for the same amount of heat delivered. This increases the Coefficient of Performance (COP, the measure of efficiency of heat pump cycle) of the system significantly.

To investigate the performance of this RPX integrated heat pump cycle, the mass flow and energy balance equations are written for this system and a comprehensive thermodynamic analysis is carried out. The results are shown in section 3.

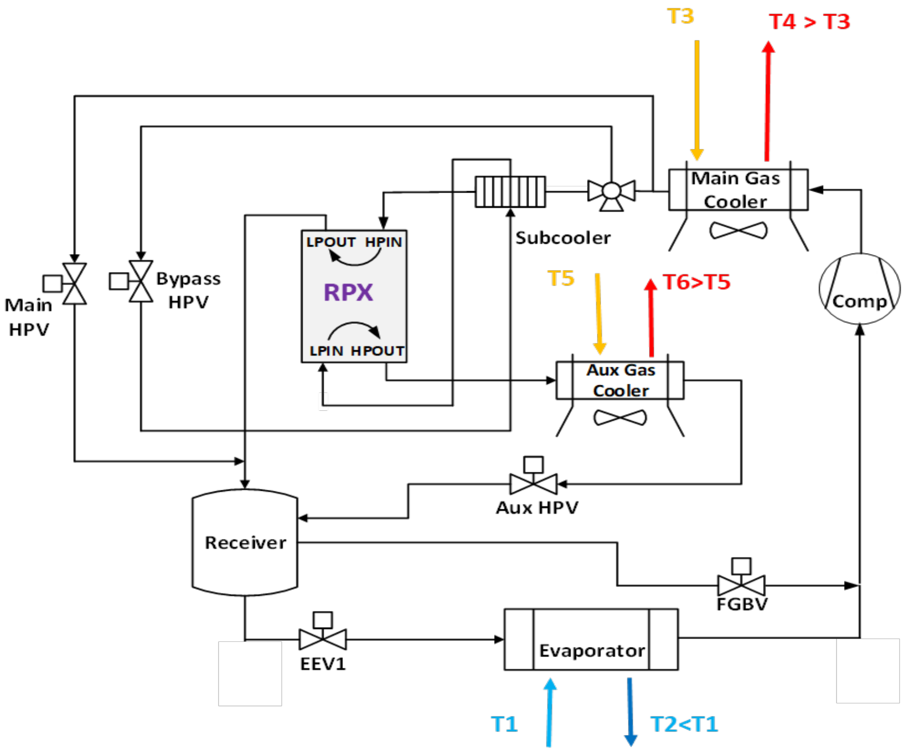

Figure 3. RPX integrated trans-critical CO2 heat pump system design.

3. Results and Discussion

Figure 4 shows the results from the exergy analysis of a standard baseline CO2 heat pump system without RPX. Fig. 4 (a) shows the variation of exergy destroyed in each of the four components of a standard heat pump system vs gas cooler exit temperature (TGC) for a system with 100 kW evaporator load, Tsource = 0 deg. C, Tevap = -2 deg. C, Tsink = $T_0 = T_{GC}$-2 deg. C. Also shown is the COP of the cycle. As discussed in section 1, the CO2 heat pump system becomes highly inefficient as gas cooler exit temperature (governed by heat pump load return temperature) increases and the COP of the system drops from over 10 to less than 2 as TGC increases from 10 to 40 deg. C. The source of this inefficiency can be analyzed by looking at the exergy destruction occurring in each of the 4 components of the system. The entropy generated in compressor, the gas cooler and high pressure expansion valve all increase with increasing TGC but the rate of increase of expansion valve exergy destruction is the highest in expansion valve. Fig. 4(b) shows the percentage contribution of exergy destroyed in each of these components as a fraction of total exergy destroyed in the system. It can be seen that the percentage contribution by expansion valve increases sharply with TGC, leading to as much as 40% of the total exergy destruction at TGC = 40 deg. C. This makes it clear that the irreversible isenthalpic expansion occurring in the high pressure expansion valve is one of the key reasons for reduced cycle COP at high gas cooler exit temperatures (i.e. load return temperatures) in trans-critical CO2 heat pump cycles.

This also indicates that a system design that can reduce this irreversibility in high pressure expansion valve, will likely improve the system efficiency significantly. This is the reason a rotary gas pressure exchanger is explored in this paper to reduce this irreversibility by means of a more “isentropic-like” expansion process that can do expansion work recovery.

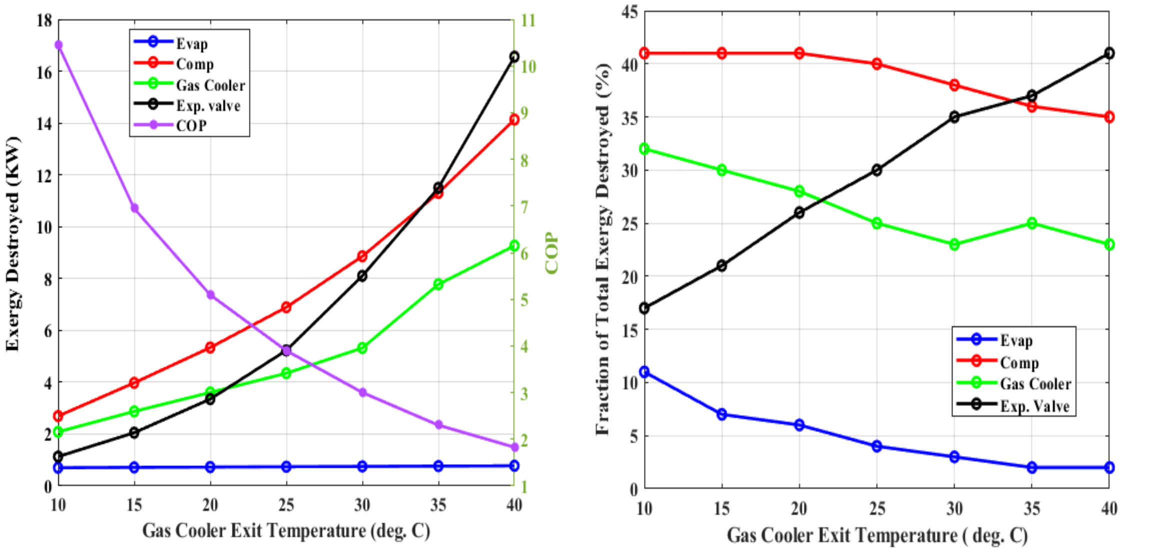

Figure 4. (a) Variation of exergy destroyed in each of the components of a standard heat pump system vs gas cooler exit temperature. Also shown is the COP of the cycle for a system with Tsource = 0 deg. C, Tevap = -2 deg. C, Tsink = $T_0 = T_{GC}$-2 deg. C. (b) Fraction of exergy destruction contributed by each component.

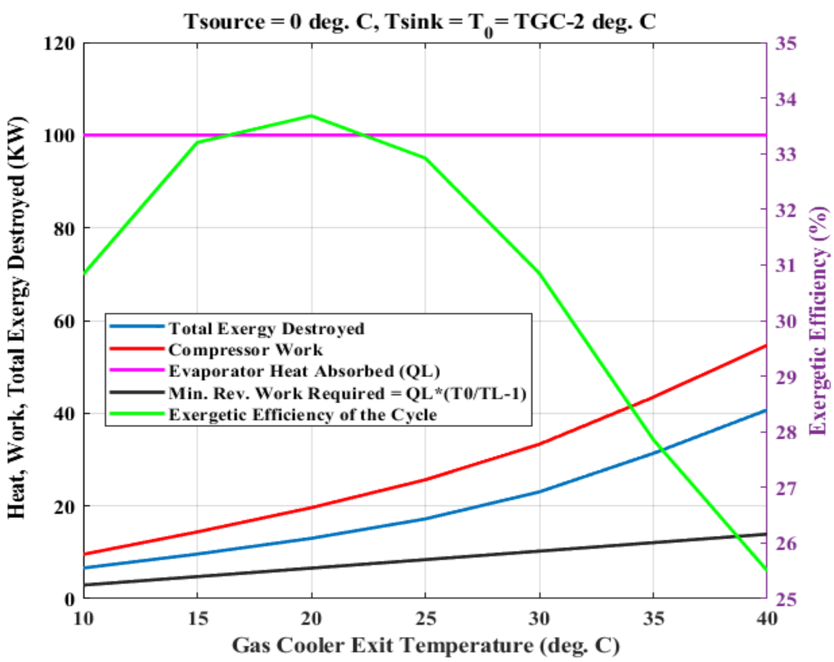

Figure 5. Total exergy destroyed and the exergetic efficiency in a standard heat pump cycle operating with Tsource = 0 deg. C, Tevap = -2 deg. C, Tsink = $T_0 = T_{GC}$-2 deg. C. The relative magnitude of exergy destruction can be compared with total exergy input through compressor work. Also shown is the minimum reversible work required to achieve this cooling. The ratio of minimum reversible work to the actual compressor work is the exergetic efficiency. The difference between the two is the total exergy destroyed across all components of the system.

Figure 5 shows the total exergy destroyed and the exergetic efficiency in a standard heat pump cycle operating with 100 kW evaporator load, Tsource = 0 deg. C, Tevap = -2 deg. C, Tsink = T0 = TGC-2 deg. C. Total exergy destroyed in the system is the sum of individual exergy destruction in each of the four components of the cycle. As expected from previous discussion, it increases with increasing TGC, reaching ~ 28.5 kW at 40 deg. C. Also plotted (black curve) is the minimum reversible work required to achieve the desired 100 kW heat absorption from 0 deg. C low temperature sink while rejecting heat to a Tsink of TGC-2 deg. C. This is $Q_L(T_0/T_L - 1)$. The actual compressor work consumed is also shown. The compressor work is same as the total exergy input to the system. The difference between compressor work and minimum reversible work is also equal to the total amount of exergy destroyed. The ratio between the minimum reversible work and the actual exergy input (compressor work) is the exergetic efficiency of the cycle, which is shown by green curve. As can be seen, the exergetic efficiency for this cycle varies between 34% and 25%, where the lowest exergetic efficiency also occurs at the highest gas cooler exit temperature.

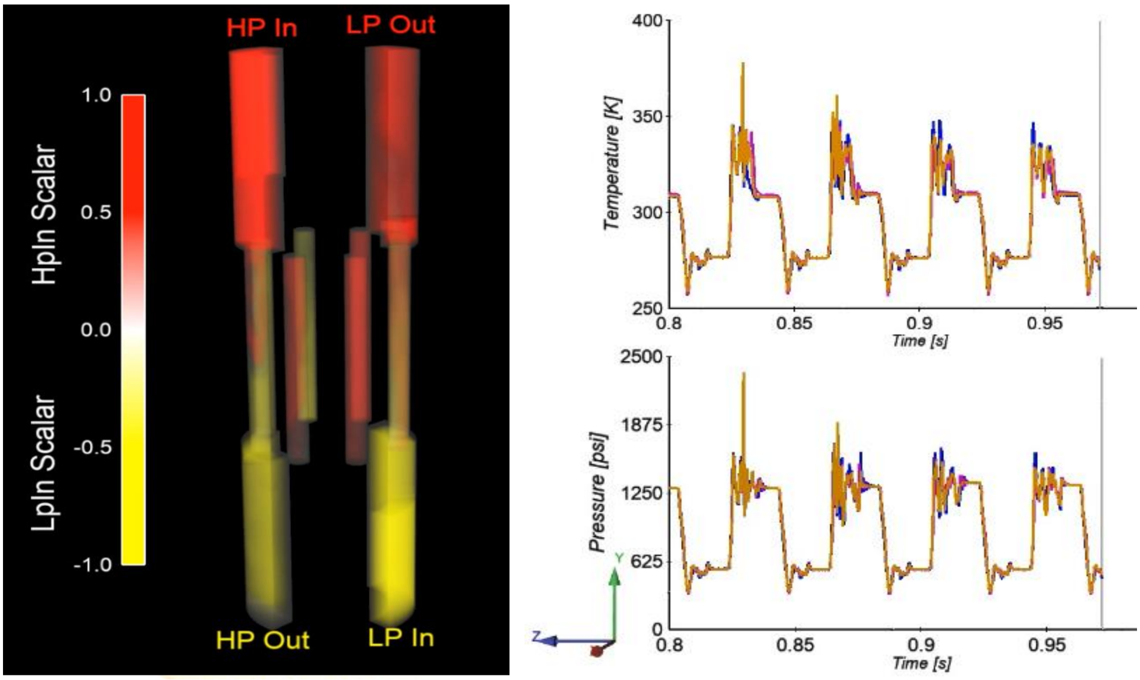

(a) (b)

Figure 6. Results from 3D flow-thermal-species transport model of RPX. (a) All high pressure supercritical CO2 mass flow entering HPin port of RPX undergoes acoustic expansion and exits through LPout port as seen by the red scalar transport. Similarly, all low pressure CO2 vapor mass flow entering LPin port undergoes acoustic compression and exits through HPout port as seen by the yellow scalar transport. (b) The pressure and temperature inside RPX port as it is cyclically exposed to the HP and LP ports.

Figure 6 shows results from the high fidelity 3D flow-species-thermal transport model of RPX. Fig. 6(a) shows the tracer transport tracked during rotation of the rotor ducts. The red tracer shows the high pressure supercritical CO2 mass flow entering the HPin port while the yellow tracer shows the low pressure CO2 vapor entering LPin port of RPX. As the duct rotates the red tracer undergoes acoustic expansion as described before and exits through the LPout port as the low pressure cold two-phase liquid-vapor. It can be seen that all the HPin flow exits through LPout port and none exits through HPout port, as desired (since otherwise it would cause a significant pass-through of low temperature enthalpy from HPin to otherwise much hotter HPout enthalpy and would degrade the performance of the cycle. Similarly all flow entering LPin port gets compressed through acoustic waves, increases in temperature (as see in Fig. 6(b)) and exits through HPout port as desired and none exits through LPout port (which would have also caused degradation of cycle performance as superheated LPin vapor would have mixed with cold two-phase liquid-vapor mixture at LPout, thus degrading the enthalpy at LPout and increasing its vapor mass fraction). Fig. 6(b) shows the time evolution of pressure and temperature in the RPX duct as it gets alternately exposed to LPin-LPout and HPin-HPout ports. The low pressure vapor filled into the duct through LPin port gets compressed to full gas cooler pressure using acoustic waves that are generated in the duct when it’s exposed to the HP ports. The HPout and HPin ports are “clocked” circumferentially to let HPout plug first discharge at high temperature before colder HPin flow starts to fill the duct and drives the remaining compressed vapor out of the duct. The temperature in the duct increases correspondingly in accordance with isentropic-like compression process (with a certain isentropic compression efficiency). This high pressure, high temperature plug of fluid is then ejected out of HPout port of RPX and goes on to reject that heat in Aux. gas cooler of system shown in Fig.3 The HPin flow expands to low pressure in an isentropic-like expansion (with certain isentropic expansion efficiency) and becomes a cold two-phase liquid-vapor mixture that exits through LPout port The vapor mass fraction (i.e. quality) of this LPout flow is lower than that produced in a standard isenthalpic expansion valve and hence it can absorb more heat per unit mass flow in the cycle. This vapor mass fraction produced through RPX expansion as the duct gets alternately exposed to HP and LP ports is shown in Fig. 7.

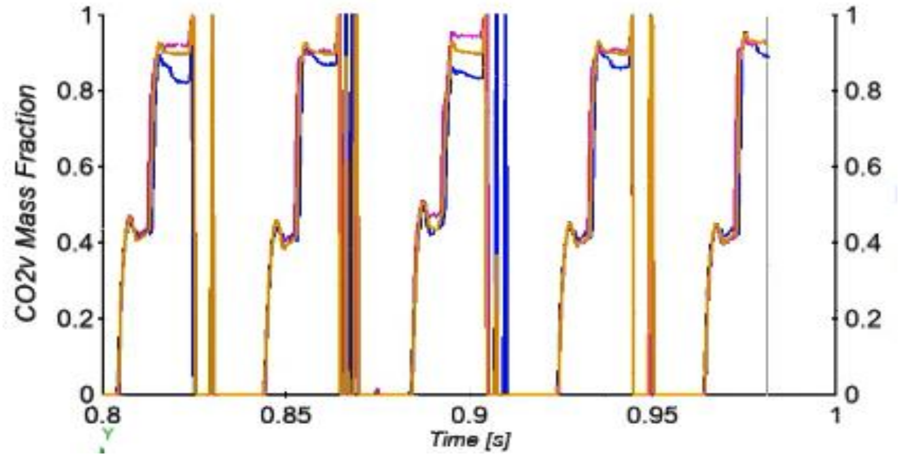

Figure 7. CO2 vapor mass fraction (i.e. quality) of the flow entering the LPin port (quality = 1 is superheated vapor) and exiting the LPout port (quality = 0.4) as cold two phase liquid-vapor mixture.

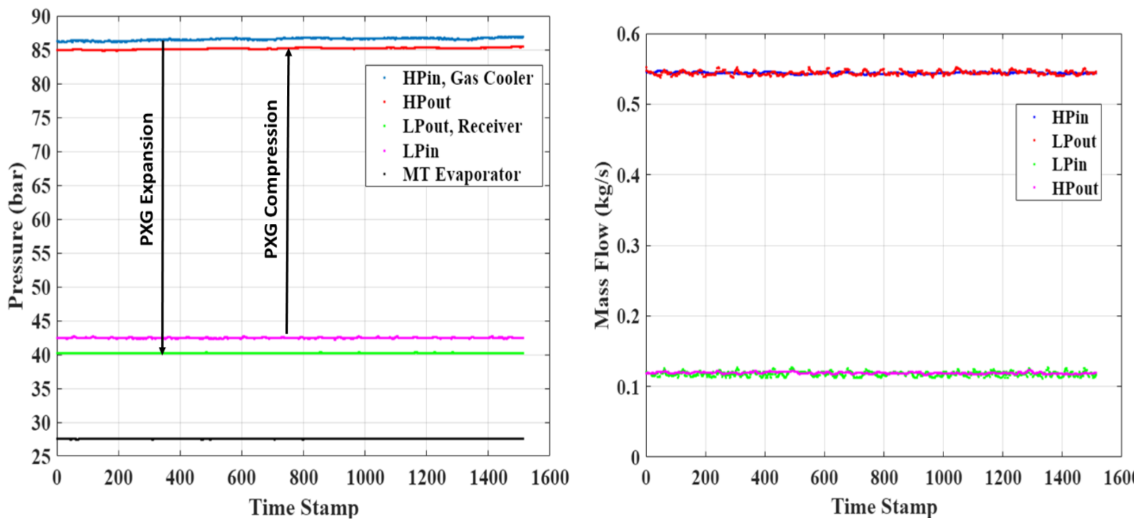

(a) (b)

Figure 8. Experimental results validating the CFD predictions of pressure exchange (a) and mass transport (b) through RPX.

Figure 8 shows the experimental validation of CFD predictions on RPX performance. Fig. 8(a) shows the that the low pressure CO2 vapor entering at LPin port is indeed compressed to the full gas cooler pressure of ~ 85 bar. There is ~ 1-2 bar pressure loss in the RPX ducts and in the piping due to viscous friction losses and inertia losses. This is the reason an Aux. gas cooler is used in addition to the primary gas cooler to reject heat of this 1-2 bar lower pressure HPout flow. Similarly the high pressure supercritical CO2 entering HPin port is expanded to low pressure (typically the receiver pressure as seen in Fig. 3). There is again ~ 1-2 bar pressure loss on the low pressure side. Fig. 8(b) shows the test data on mass flows at the 4 ports of RPX. It can be seen that all LPin flow entering RPX exits through HPout port at high pressure as predicted by the CFD model.

Similarly, all HPin flow exits at low pressure through LPout port of RPX. This ensures optimal performance of RPX and reduced "mass mixing" and "enthalpy mixing".

Having validated the gas dynamics, species and enthalpy transport through RPX, it is then integrated with the heat pump system model as shown in Fig. 3 and the system level analysis is carried out as described in section 2. The results of this analysis are shown in Fig. 9 and Fig. 10. Fig. 9 shows heat absorbed, heat delivered in main gas cooler, heat delivered in Aux. gas cooler and compressor work done for the RPX integrated system and its comparison with a std. heat pump cycle. The variation with evaporating temperature for a constant gas cooler exit temperature of 40 deg. C and constant gas cooler pressure of 100 bar is shown. It can be seen that both the systems provide same heat in the main gas cooler and consume the same amount of compressor work. However, the RPX system provides an additional heat through Aux. gas cooler, thus increasing heating COP. As can be seen, due to its subcooling mechanism as discussed in section 2 and Fig. 3, RPX based system also provides more cooling capacity (higher heat absorbed in evaporator), in addition to higher heating capacity, when compared to the std. heat pump cycle.

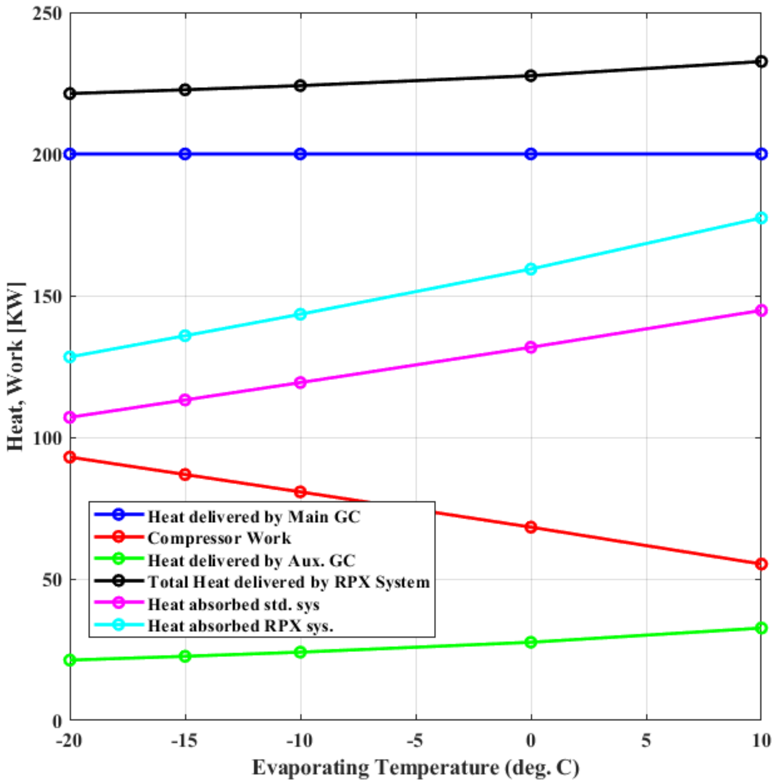

Figure 9. Heat absorbed, heat rejected and work done in RPX integrated trans-critical CO2 heat pump system and its comparison with std. cycle. Gas cooler exit temperature = 40 deg. C, gas cooler pressure = 100 bar.

Fig. 10 shows the increase in COP of the heat pump cycle provided by RPX based system when compared with std. heat pump cycle. This increase in efficiency, primarily comes from additional heating load delivered by RPX system for same amount of compressor work consumed. The reason for this is the "free subcooling" provided by RPX system through expansion work recovery. This expansion work recovery in RPX reduces the exergy destruction that was seen in the std. cycle (Fig. 4, Fig. 5) and increases the thermodynamic potential to lift the low grade heat from source temperature to sink temperature. It can be seen that RPX can increase the COP of the system by up to 16% at 10 deg. C evaporating temperature and 40 deg. C gas cooler exit temperature, which is a common condition for district heating and industrial heat pumps

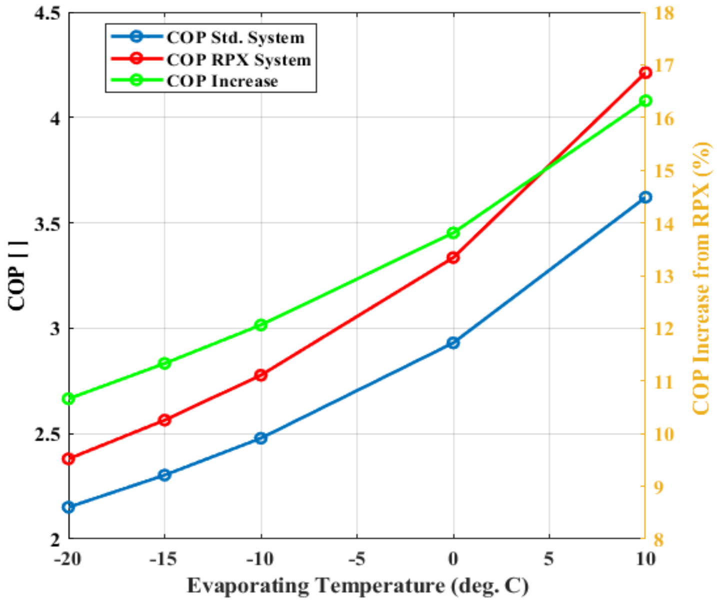

Figure 9. COP and COP Lift provided by RPX integrated trans-critical CO2 heat pump cycle compared to a standard heat pump cycle.

Thus this novel RPX based heat pump cycle presents a fundamentally new way to design heat pump systems by performing a “full differential pressure expansion work recovery” in order to reduce the exergy losses, something that was not seen in the state of the art until now.

One question that may be asked is how does RPX technology as an expansion work recovery machine compare to a turbo-compressor (a turbine and a compressor mechanically coupled, e.g. on the same shaft or through gearing mechanism) ? We investigated the performance of an "Idealized Expansion Work Recovery Machine" like an idealized turbo-compressor without any losses (e.g. aerodynamic or mechanical losses). Depending on the range of boundary conditions explored, the efficiency of the RPX based cycle is in the range of 70%-80% of the efficiency of such an ideal turbo-compressor based cycle. However, there are several aerodynamic and thermo-mechanical loss mechanisms in trans-critical CO2 expansion and compression that reduce the efficiency of the "Real" turbo-compressor from that of an ideal one. Many of these have been highlighted in literature (e.g. [6]) and the real performance of a turbo-compressor lies somewhere in the range of 60%-80% of the ideal performance prediction. In that regard the performance of RPX is comparable if not better to that of a turbo-compressor. Additionally, RPX is relatively a much simpler machine with only 1 moving part and 3 stationary parts compared to tens of individual components (bearings, seals, blades, vanes, nozzles, volutes, shafts etc.) which introduce additional mechanical losses, rotordynamic instabilities, off-design aerodynamic performance drops, reliability issues, manufacturing complexities and cost constraints. In this regard RPX is a much more simple, reliable and efficient machine.

4. Conclusions

Heat pumps with CO2 as the working fluid provide unique advantages and facilitates transition away from global warming hydrofluorocarbons (HFC) towards natural refrigerants with ultra-low global warming potential. However molecular structure of CO2 causes the heat rejection pressure to be much higher compared to HFCs, resulting in lower efficiency of the cycle at high gas cooler exit temperatures. Exergy and second law analysis indicates that largest fraction of exergy is destroyed during the throttling process over high differential pressure between heat source and sink. To increase exergetic efficiency, this paper presented a novel rotary gas pressure exchanger (RPX), which allows expansion work recovery using direct fluid-to-fluid contact acoustic pressure exchange between high pressure supercritical CO2 and low pressure gaseous CO2. RPX facilitates both, the compression and the expansion using acoustic waves generated in a compact high speed axially ducted rotary machine. RPX can compress a large fraction of the low pressure CO2 vapor for free without consuming any external mechanical or electrical energy, but rather through the expansion work recovery. This expansion work recovery, not only reduces the exergy destruction during expansion process but also provided free subcooling, thus reducing total system mass flow for same amount of total heat delivered or delivering more heat for same amount of compressor work consumed. Test results demonstrate more than 95% pressure recovery coefficient and no-pass through characteristic of mass transport through RPX. The paper presented a novel RPX integrated heat pump architecture that shows up to 16% COP improvement achieved through this reduction in exergetic efficiency of the cycle. Such an RPX integrated heat pump architecture has a great potential to facilitate efficient decarbonization of district and industrial process heat using ultra-low global warming refrigerants like CO2.

References

[1] Barta, R.B., Groll, E.A., Ziviani, D., 2021. Review of stationary and transport CO2 refrigeration and air conditioning technologies. Applied Thermal Engineering 185, 116422.

[2] Elbarghthi, A.F.A., Hafner, A., Banasiak, K., Dvorak, V., 2021. An experimental study of an ejector-boosted transcritical R744 refrigeration system including an exergy analysis. Energy Conversion and Management 238, 114102.

[3] Kakuda, M., Nagata, H., Ishizono, F., 2009. Development of a scroll expander for the CO2 refrigeration cycle. HVAC&R Research 15(4), 771-783.

[4] Kohsokabe, H., Funakoshi, S., Tojo, K., Nakayama, S., Kohno, K., 2006. Basic operating characteristics of CO2 refrigeration cycles with expander-compressor unit. International Refrigeration and Air Conditioning Conference, Purdue University, West Lafayette, IN, 8p.

[5] Thatte A., 2019, "Transcritical/ Supercritical CO2 Recompression Brayton Cycle using A Novel Rotary Liquid Piston Compressor", GT2019-91088.

[6] Rafiee S., 2025, " Comprehensive study on the design and analysis of supercritical carbon dioxide (sCO2) radial outflow turbines (ROTs), focusing on tip clearance effects, loss correlations, and performance evaluation", *Applied Thermal Engineering*, Vol. 272, 126399.